

Provided for non-commercial research and education use.
Not for reproduction, distribution or commercial use.



(This is a sample cover image for this issue. The actual cover is not yet available at this time.)

This article appeared in a journal published by Elsevier. The attached copy is furnished to the author for internal non-commercial research and education use, including for instruction at the authors institution and sharing with colleagues.

Other uses, including reproduction and distribution, or selling or licensing copies, or posting to personal, institutional or third party websites are prohibited.

In most cases authors are permitted to post their version of the article (e.g. in Word or Tex form) to their personal website or institutional repository. Authors requiring further information regarding Elsevier's archiving and manuscript policies are encouraged to visit:

<http://www.elsevier.com/copyright>



Contents lists available at SciVerse ScienceDirect

Computational Materials Science

journal homepage: www.elsevier.com/locate/commatsci

Nonlinear flow-induced vibration of a SWCNT with a geometrical imperfection

A. Farshidianfar^a, P. Soltani^{a,*}^a Department of Mechanical Engineering, Ferdowsi University of Mashhad, Mashhad, Iran

ARTICLE INFO

Article history:

Received 23 July 2011

Received in revised form 8 August 2011

Accepted 15 August 2011

Keywords:

Flow-induced vibration

Nanotube

Imperfection

Nonlinear vibration

Nonlocal theory

Pasternak foundation

Perturbation method of multi scales

ABSTRACT

Based on the nonlocal continuum theory, transverse vibration of a single-walled carbon nanotube (SWCNT) conveying fluid with immovable support conditions is investigated. Unlike previous similar studies, the SWCNT is assumed to be not perfectly straight and initially includes a slight geometrical curvature as an imperfection. The SWCNT is assumed to be embedded in a Pasternak-type foundation. Hamilton's principle is applied to drive an efficient governing equation of motion, which covers stretching, large deformation, and imperfection nonlinearities. The perturbation method of multi scales (MMS) is applied and the nonlinear flow-induced frequency ratio is analytically calculated. The obtained results reveal that the imperfection of the nanotube at high flow velocities makes the model severely nonlinear, especially when considering the nonlocal effects. A noteworthy observation is that the nonlinear flow-induced frequency ratio is decreased as the imperfection of the nanotube increases. Whereas through a parametric study, the effects of the flow velocity, nonlocal parameter, the stiffness of the elastic foundation, and the boundary conditions (BCs) on this frequency reduction are calculated and discussed widely.

© 2011 Elsevier B.V. All rights reserved.

1. Introduction

A needle-like carbon nanostructure with a hollow cylindrical shape was first discovered and reported by Iijima [1]. electrical, chemical and physical properties of carbon nanotubes (CNTs) made them appropriate for many applications in nanotechnology and nanoengineering. Several nano-electro-mechanical systems (NEMS) work on the basis of the properties of nanotubes while more innovative potential applications are proposed for the future. Nano-sensors [2–4], nano-resonators [5,6], nano-switches [7,8], nano-resistors [9,10], nano-motors [11,12], and nano-robots [13] are some interesting examples of the recent uses of the CNTs. Owning mainly to perfectly cylindrical channels and remarkable mechanical properties, nanotubes embrace variety applications as nano-containers, nano-channels, and nano-pipes for conveying fluid and gas [14–17]. In this fashion, CNTs can find uses in artificial blood vessels and drug-delivery systems (DDSs) in the field of nanobiotechnology [18,19]. A CNT-based DDS is generally designed to carry drugs and deliver them to a target cell. For instance, in cancer therapy, CNTs can be used as nano-needles to transport the drug agents directly into the tumor cells. This targeted delivery improves the pharmacological and therapeutic profile of drugs with a consequent reduction of undesirable side effects [20,21]. To employ nanotubes in such applications and to develop their usage, we need to explore the dynamic nature of, and the impact

of flow-induced vibrations in, these nano-pipes. Molecular dynamics (MD) simulations using empirical potentials can be used to model the interaction between the flowing fluid and the nanotube but these atomic-base simulations are still prohibitive, time-consuming and formidable for nanostructures with large numbers of atoms. Recently, continuum mechanics models have been effectively and successfully used to simulate the flow-induced vibration of CNTs. Euler–Bernoulli continuum theory has been applied widely to investigate flow-induced vibration, instability, and dynamic behavior of nanotubes in several papers [16,22–26]. Chang and Lee [27] applied Timoshenko continuum theory to explore the flexural vibration of a single-walled carbon nanotube (SWCNT) conveying fluid and the effects of the fluid flow on the resonant frequencies were explained. As the size of CNTs is on the nano-scale, the local continuum theories may not predict the mechanical behavior of CNTs accurately. Hence, the above-mentioned local theories should be modified by using Eringen's nonlocal theory [28]. This theory contains information about the long-range forces between atoms and the internal length scale and consequently, simulates the vibrational behavior of CNTs more precisely. Wang [29] used a nonlocal Euler–Bernoulli continuum model for a double-walled carbon nanotube (DWCNT) conveying fluid and obtained the effects of the small length scale on resonant frequency and critical flow velocity. Lee and Chang developed a nonlocal elastic theory for a fluid-conveying SWCNT [30], and DWCNT [31] to study the influence of the nonlocal parameter on the vibration and instability of nanotubes. Moreover, the effects of temperature change [32] and the visco-elastic foundation [33] on the vibrations

* Corresponding author.

E-mail addresses: soltanip2@asme.org, payam.soltani@gmail.com (P. Soltani).

and instability of a SWCNT conveying fluid were investigated using nonlocal Euler–Bernoulli elastic theory. Since the previous experiments confirm that the deformation nature of nanostructures is intrinsically nonlinear, especially for large external forces and/or large deflections [34–36], the linear modeling of the vibrational behavior of CNTs may cause some inaccuracy in the results. However, all of the above studies are limited to linear vibration behavior of CNTs, while the nonlinear one has been rarely investigated. Rasekh and Khadem [37] introduced a nonlinear model for the flow-induced vibration of a SWCNT conveying fluid embedded in a Winkler-type foundation. The model was developed on the basis of the local Euler–Bernoulli continuum theory and stretching nonlinearity was taken into account. The relationship between the nonlinear resonant frequency and the vibration amplitude was derived using the perturbation method and the effects of parameters such as the flow velocity, surrounding elastic medium, mass and aspect ratios of nanotube were considered.

1.1. Motivation

All previous papers simulate the CNT as an entirely straight and perfect beam structure. Although the photos taken by transmission electron microscopes (TEM) show that the CNTs usually exhibit a certain degree of “waviness” along their length, which influences their dynamical and mechanical behavior efficiently [38,39]. Lately, the flow-induced vibrations of a curved SWCNT have been considered by Xia and Wang [40] through a linear elastic model and the linear resonant frequencies have been compared with those of straight CNTs. Ghavanloo et al. [41] studied the effects of the visco-elastic medium on the resonant frequency of a semicircular SWCNT. In this research, the nanotube has been assumed to have a circularly curved shape and is modeled as a linear and local circular Euler–Bernoulli beam with an inextensible centerline. However, the immovable support conditions and the extensible assumption for the centerline which make the model nonlinear, represent a more practical situation than the inextensible condition [42] and cause the centerline strain of the nanotube to be taken into account.

Due to the lack of research in these areas, the motivation for this work is to exploit an efficient nonlinear vibrational model for a fluid-conveying SWCNT with a geometrical imperfection. The imperfection is assumed to be as a slight curvature initially and the presented model accounts for the effects of large deformations and the immovable boundary conditions, simultaneously. The foundation around the nanotube is modeled as a Pasternak-type foundation and three classical boundary conditions (BCs) are applied to investigate the effects of the support stiffness. According to each specified BC, the imperfection of the SWCNT is chosen separately. Using Hamilton’s principle, the nonlinear governing equation of motion is derived based on the nonlocal continuum theory. The perturbation method of multiple scales (MMS) is applied to solve the nonlinear equation which contains both cubic and quadratic nonlinear terms and an explicit expression is obtained for the nonlinear flow-induced frequency ratio. The effects of the imperfection on the model’s nonlinearity and the nonlinear frequency ratio are explained and the role of key parameters such as flow velocity, nonlocal parameter, stiffness of the foundation, and BCs is analyzed.

2. The nonlinear model for a SWCNT conveying fluid with an initial imperfection

In this section, on the basis of the nonlocal Euler–Bernoulli continuum theory, the governing equation of motion for a SWCNT conveying fluid with an initial imperfection will be given. Consider a

fluid-conveying SWCNT modeled as a nano-pipe of length L , mean radius R_{ave} and constant thickness h that rests on a Pasternak-type elastic foundation. A Pasternak foundation model describes a clarified simulation for an elastic medium using a shear layer with linear elastic stiffness. Recently, some papers applied the Pasternak model for the foundation of nano-materials and nanotubes successfully [43–45]. In this kind of foundation model two different constants express the stiffness of the medium, and this is why it is also called the two-parameter foundation model. Here, k_w and k_c represent the elastic stiffness and the shear stiffness of the elastic foundation respectively. The CNT is assumed to have an initial geometrical imperfection with the initial imperfection function $w_0(x)$ (Fig. 1). The rise of the imperfect nanotube R is defined as the maximum height of the midline of the model from the x axis and is assumed to be small with respect to the length of the nanotube L . This means that the imperfection does not affect the bending moment and the fluid flow [46] and needs to satisfy the BCs of the CNT.

To derive the equation of motion, the energy principle and the variational approach will be used. To this end, based on the immovable end conditions the kinetic energy due to the internal fluid flow T_f is approximated as follows:

$$T_f = \frac{1}{2} m_f \int_0^L \left[\left(\frac{\partial w}{\partial t} + V \frac{\partial w}{\partial x} \right)^2 + \left(\frac{\partial u}{\partial t} \right)^2 \right] dx, \quad (1)$$

m_f is the mass of fluid per unit length, u and w are the longitudinal and transverse displacement of the SWCNT and V shows the steady flow velocity. The kinetic energy corresponding to the motion of the SWCNT is:

$$T_c = \frac{1}{2} m_c \int_0^L \left[\left(\frac{\partial w}{\partial t} \right)^2 + \left(\frac{\partial u}{\partial t} \right)^2 \right] dx, \quad (2)$$

where m_c stands for the mass of the nanotube per unit length. The total kinetic energy can be defined as $T = T_f + T_c$ and its variation δT is obtained as:

$$\begin{aligned} \delta T = \delta T_f + \delta T_c = m_f \int_0^L \left\{ \delta \left(\frac{\partial w}{\partial t} + V \frac{\partial w}{\partial x} \right) \left(\frac{\partial w}{\partial t} + V \frac{\partial w}{\partial x} \right) \right. \\ \left. + \left(\delta \left(\frac{\partial u}{\partial t} + V \frac{\partial u}{\partial x} \right) \left(\frac{\partial u}{\partial t} + V \frac{\partial u}{\partial x} \right) \right\} dx + m_c \right. \\ \left. \times \int_0^L \left(\frac{\partial w}{\partial t} \delta \left(\frac{\partial w}{\partial t} \right) + \frac{\partial u}{\partial t} \delta \left(\frac{\partial u}{\partial t} \right) \right) dx. \end{aligned} \quad (3)$$

Based on the Euler–Bernoulli continuum theory, the displacement field of the model is expressed as:

$$u(x, y, t) = u(x, t) - z \cdot \frac{\partial w}{\partial x}, \quad (4)$$

$$w(x, y, t) = w(x, t),$$

where z is the distance from the neutral axis of the nanotube. By assuming large deformation of the imperfect SWCNT but small strains, the nonzero component of the von-Karman strain is approximately expressed as [47]:

$$\varepsilon_{xx} = \frac{\partial u}{\partial x} + \frac{1}{2} \left(\frac{\partial w}{\partial x} \right)^2 + \frac{\partial w_0}{\partial x} \frac{\partial w}{\partial x}. \quad (5)$$

The variation of the strain energy for the one-dimensional stress–strain field is derived using Eq. (5) and the variational rules.

$$\begin{aligned} \delta U = \int_V \sigma_x \delta \varepsilon_x dV \\ = \int_0^L \left[N_x \left(\delta \frac{\partial u}{\partial x} + \frac{\partial w}{\partial x} \cdot \delta \frac{\partial w}{\partial x} + \frac{\partial w_0}{\partial x} \cdot \delta \frac{\partial w}{\partial x} \right) - M_x \delta \left(\frac{\partial^2 w}{\partial x^2} \right) \right] dx, \end{aligned} \quad (6)$$

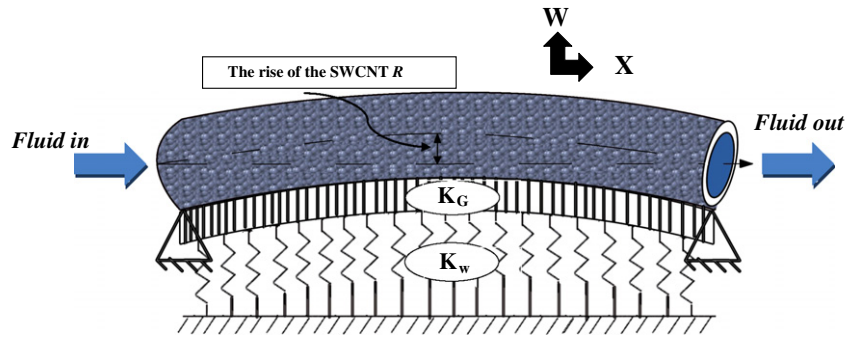


Fig. 1. Schematic diagram of a SWCNT conveying fluid with a geometrical imperfection.

σ_x is the longitudinal bending stress. N_x and M_x are the stress resultants defined as follows:

$$N_x \equiv \int_A \sigma_x dA, \quad M_x \equiv \int_A \sigma_x \cdot z \cdot dA, \quad (7)$$

where A is the cross-sectional area of the SWCNT.

The virtual work δW^{ext} done by the external transverse forces F^{ext} exerted on the nanotube by the Pasternak elastic foundation can be calculated as:

$$\delta W^{ext} = \int_0^L F^{ext} \cdot \delta w \cdot dx = \int_0^L \left[-k_w \cdot w + k_G \frac{\partial^2 w}{\partial x^2} \right] \cdot \delta w \cdot dx. \quad (8)$$

In the above equation the viscosity of the flowing fluid through the nanotube and the corresponding external work have been ignored as indicated by Wang and Ni [48].

Using the dynamic version of the principle of virtual displacements or Hamilton's principle [49],

$$\int_{t_1}^{t_2} (\delta T + \delta U - \delta W^{ext}) dt = 0, \quad (9)$$

substituting Eqs. (3), (6), and (8) into Eq. (9), integrating by parts and setting the coefficients of δu and δw zero, lead to the equations of motion as

$$\delta u: \quad m_f(-\ddot{u} - 2V\dot{u}' - V^2u'') - m_c\ddot{u} + N_x' = 0, \quad (10)$$

$$\begin{aligned} \delta w: \quad & m_f(-\ddot{w} - 2V\dot{w}' + V^2w'') - m_c + (N_x w')' + (N_x W_0)' \\ & + M_x'' - k_w w + k_G w'' - Pw'' \\ & = 0, \end{aligned} \quad (11)$$

where prime and overdot denote the derivatives with respect to x and t , respectively. For slender CNTs with immovable end conditions (i.e. $u(0, t) = u(L, t) = 0$), the variation of the longitudinal inertial forces can be neglected and as a result:

$$\frac{\partial N_x}{\partial x} \approx 0. \quad (12)$$

By substituting Eqs. (7) and (4) into Eq. (12) and using immovable end conditions, the following relation between the longitudinal displacement u and the transverse displacement w is calculated:

$$\begin{aligned} u = & -\frac{1}{2} \int_0^x \left[\frac{1}{2}(w')^2 + \frac{dw_0}{dx} \cdot w' \right] dx + \frac{x}{L} \\ & \times \int_0^L \left[\frac{1}{2}(w')^2 + \frac{dw_0}{dx} \cdot w' \right] dx. \end{aligned} \quad (13)$$

Hence, N_x can be easily calculated from Eqs. (5), (7), and (13):

$$N_x = \frac{EA}{L} \left[\int_0^L \left(\frac{1}{2}(w')^2 + w' \frac{dw_0}{dx} \right) dx \right], \quad (14)$$

where E is the Young's modulus of the SWCNT.

The nonlocal continuum theory, introduced by Eringen in 1983, represents a more precise constitutive rule for small-scale structures in comparison with the common local elastic theories. This theory states that the stress tensor at a reference point in an elastic medium depends not only on the strains at that point but also on the strains at all other points in the body [43]. This definition of nonlocal elasticity is based on lattice dynamics and observations on phonon dispersion. The nonlocal constitutive equation for the uniaxial bending stress state forms as [50]

$$M_x - (e_0 a)^2 \frac{\partial^2 M_x}{\partial x^2} = EI \kappa(x, t). \quad (15)$$

Here, $\kappa(x, t)$ denotes the bending curvature, and the parameter $e_0 a$ shows the small-scale effect which is called the nonlocal parameter. In fact, the parameter e_0 is estimated such that the relations of the nonlocal elasticity model could provide a satisfactory approximation of atomic dispersion curves of plane waves with those of atomic lattice dynamics, and a represents an internal length such as lattice parameter, granular size, or distance between C-C bonds[44].

Based on the large deflection deformation, the relation between the bending curvature $\kappa(x, t)$ and the nanotube transverse deflection $w(x, t)$ is defined as:

$$\kappa = \frac{-w''}{[1 + w'^2]^{\frac{3}{2}}} \cong -w''[1 - r_0 w'^2 + \dots], \quad r_0 = \frac{3}{2}. \quad (16)$$

Substituting Eq. (16) into Eq. (15) yields:

$$M_x - (e_0 a)^2 \frac{\partial^2 M_x}{\partial x^2} = -EI w'' [1 - r_0 w'^2 + \dots]. \quad (17)$$

Using Eqs.(17) and (11) at the same time with omitting the resultant stress M_x , the nonlinear governing equation of motion for a fluid-conveying SWCNT with an imperfection is obtained:

$$\begin{aligned} (m_f + m_c)\ddot{w} + 2m_f V \cdot \dot{w}' + m_f V^2 w'' + EI w'''' - NL_1 + k_w w \\ - k_G w'' - NL_2 - (e_0 a)^2 [(m_f + m_c)\ddot{w}'' + 2m_f V \cdot \dot{w}''' + m_f w'''' \\ + EI w'''' + k_w w - k_G w'' - NL_2] \\ = 0, \quad NL_1 \equiv -2r_0 EI (w' w''') \text{ and } NL_2 \\ \equiv N_x \cdot [w'' + \frac{d^2 w_0}{dx^2}]. \end{aligned} \quad (18)$$

In the above equation, the nonlinearities of the model are summarized as NL_1 and NL_2 . NL_1 deals with nonlinearity due to the large deformations while NL_2 represents the nonlinearities caused by the axial stretching and the imperfection of the nanotube.

In this model, three standard BCs are employed to demonstrate the effects of end stiffness on the vibrational characteristics of the imperfect SWCNT conveying fluid. The pinned–pinned (P–P), clamped–pinned (C–P), and the clamped–clamped (C–C) conditions can be defined as follows:

P–P conditions:

$$\begin{aligned} w(0, t) = w(L, t) = 0, \\ w''(0, t) = w''(L, t) = 0. \end{aligned} \quad (19)$$

C–P conditions:

$$\begin{aligned} w(0, t) = w(L, t) = 0, \\ w'(0, t) = w'(L, t) = 0. \end{aligned} \quad (20)$$

C–C conditions:

$$\begin{aligned} w(0, t) = w(L, t) = 0, \\ w'(0, t) = w'(L, t) = 0. \end{aligned} \quad (21)$$

For convenience, these equations can be made dimensionless by using the following definitions:

$$\begin{aligned} W = \frac{w}{r}; \quad W_0 = \frac{w_0}{r}; \quad X = \frac{x}{L}; \quad T = \omega_0 t; \\ \omega_0 = \left(\frac{EI}{m_f + m_c} \right)^{\frac{1}{2}}; \quad v = \left(\frac{m_f}{EI} \right)^{\frac{1}{2}} \cdot V \cdot L; \\ K_w = \frac{k_w L^4}{EI}; \quad K_G = \frac{k_G L^2}{EI}; \quad m = \frac{m_f}{m_f + m_c}; \quad \mu = \frac{e_0 a}{L}; \end{aligned} \quad (22)$$

where W is the dimensionless transverse displacement parameter, X shows the dimensionless longitudinal coordinate, and r is the radius of the gyration of cross section. v represents the dimensionless flow velocity parameter and K_w, K_G symbolize the dimensionless parameters for elastic constant and shear constant of the foundation. m is defined as the dimensionless mass ratio.

Substituting the dimensionless parameters (Eq. (22)) into Eq. (18), the nonlinear dimensionless form of the governing equation is obtained:

$$\begin{aligned} \frac{\partial^2 W}{\partial T^2} + 2\sqrt{m} \frac{\partial^2 W}{\partial T \partial X} + (v^2 - K_G) \frac{\partial^2 W}{\partial X^2} + \frac{\partial^4 W}{\partial T^4} - \overline{NL}_2 + K_w W \\ - \overline{NL}_1 \\ - (e_0 a)^2 \left[\frac{\partial^4 W}{\partial X^2 \partial T^2} + 2\sqrt{m} \frac{\partial^4 W}{\partial T \partial X^3} + (v^2 - K_G) \frac{\partial^4 W}{\partial X^4} - \overline{NL}_2 + K_w \frac{\partial^2 W}{\partial X^2} \right] \\ = 0, \end{aligned} \quad (23)$$

where

$$\begin{aligned} \overline{N} \equiv \frac{r^2 EA}{L^2} \int_0^L \left(\frac{1}{2} \left(\frac{\partial W}{\partial X} \right)^2 + \frac{\partial W}{\partial X} \frac{dW_0}{dX} \right) dX, \\ \overline{NL}_1 \equiv 2r_0 r \left(\left(\frac{\partial^2 W}{\partial X^2} \right)^2 + \frac{\partial W}{\partial X} \frac{\partial^3 W}{\partial X^3} \right), \\ \overline{NL}_2 \equiv \frac{r \cdot \overline{N}}{L^2} \left(\frac{\partial^2 W}{\partial X^2} + \frac{d^2 W_0}{dX^2} \right). \end{aligned} \quad (24)$$

Furthermore, the dimensionless forms of the BCs are easily calculated as:

Dimensionless P–P conditions:

$$\begin{aligned} W(0, T) = W(1, T) = 0, \\ \frac{\partial^2 W(0, T)}{\partial X^2} = \frac{\partial^2 W(1, T)}{\partial X^2} = 0. \end{aligned} \quad (25)$$

Dimensionless C–P conditions:

$$\begin{aligned} W(0) = W(1) = 0, \\ \frac{\partial W(0, T)}{\partial X} = \frac{\partial^2 W(1, T)}{\partial X^2} = 0. \end{aligned} \quad (26)$$

Dimensionless C–C conditions:

$$\begin{aligned} W(0, T) = W(1, T) = 0, \\ \frac{\partial W(0, T)}{\partial X} = \frac{\partial W(1, T)}{\partial X} = 0. \end{aligned} \quad (27)$$

3. Solution methodology

In order to convert the governing equation of motion Eq. (23) into an ordinary differential equation of motion, the Galerkin method is employed. Hence, the dimensionless transverse displacement can be simplified as:

$$W(X, T) = \sum_{i=1}^n Y_i(T) \cdot \varphi_i(X), \quad (28)$$

where n is the number of degrees of freedom, $\varphi_i(X)$ is the i^{th} eigenfunction of the CNT, and $Y_i(T)$ is the i th time-dependent deflection parameter of the model. Based on a single degree of freedom model of the beams Eq. (23) can be solved with appropriate accuracy [51] and the solution is constructed by expressing the deflection function $W(X, T)$ as the product of two separate functions:

$$W(X, T) = Y(T) \cdot \varphi(X), \quad (29)$$

$Y(T)$ is the dynamical transverse response of the model while the shape function $\varphi(X)$ is related to the boundary conditions. Meanwhile, the dimensionless imperfection function $W_0(X)$ should satisfy the corresponding BCs and has been assumed as a harmonic function of X in this paper. Hence, for the P–P boundary condition, the mode shape of the model for the first mode of vibration is:

$$\varphi(X) = \sqrt{2} \sin(\pi X), \quad (30)$$

and the corresponding imperfection function $W_0(X)$ satisfying the P–P condition should be:

$$W_0(X) = \mathfrak{R} \sin(\pi X), \quad (31)$$

where \mathfrak{R} is the maximum dimensionless height from the x axis or “the dimensionless rise” of the imperfect SWCNT.

For C–P condition, the mode shape of vibration is

$$\begin{aligned} \varphi(X) = \cos(\beta X) - \cosh(\beta X) - \sin(\beta X) + \sinh(\beta X), \\ \beta = 3.926602, \end{aligned} \quad (32)$$

with the following imperfection function:

$$W_0(X) = \frac{\mathfrak{R}}{2\pi} \sin(1.43\pi X) - 1.43\pi \cdot \cos(1.43\pi X) + 1.43\pi(1 - X). \quad (33)$$

And finally, the C–C condition has a mode shape as:

$$\begin{aligned} \varphi(X) = \cos(\beta X) - \cosh(\beta X) - \sin(\beta X) + \sinh(\beta X), \\ \beta = 4.730041, \end{aligned} \quad (34)$$

and the imperfection function as:

$$W_0(X) = \frac{\mathfrak{R}}{2} \cos(1 - 2\pi X). \quad (35)$$

By substituting Eq. (29) into Eq. (23) and using the appropriate mode shape $\varphi(X)$ and imperfection function $W_0(X)$ for each kind of boundary conditions, the nonlinear ordinary differential equation of motion is concluded:

$$A_{-2} \frac{d^2 Y}{dT^2} + A_{-1} \frac{dY}{dT} + A_1 Y + A_2 Y^2 + A_3 Y^3 = 0. \quad (36)$$

A_{-2}, A_{-1}, A_1, A_2 and A_3 are parametric constants which can be defined regarding to the BCs as follows:

For P–P conditions:

$$\begin{aligned} A_{-2} &= 1 + (\mu\pi)^2; \\ A_{-1} &= 0; \\ A_1 &= (k_w + K_G - p)\pi^2(1 + \mu^2\pi^2L^4) - v^2\pi^2(1 + \mu^2L^2) \\ &\quad + \pi^4(1 + \frac{\mathfrak{R}^2}{2}(1 + \mu\pi^2L^2)); \\ A_2 &= \frac{3\sqrt{2}}{4}\pi^4 \mathfrak{R}(1 + (\mu\pi)^2) - \frac{8\sqrt{8}\pi^3}{3}r.r_0; \\ A_3 &= \frac{\pi^4}{2}(1 + (\mu\pi)^2). \end{aligned} \quad (37)$$

For C–P conditions:

$$\begin{aligned} A_{-2} &= 1 + 11.50\mu^2, \\ A_{-1} &= (3.32 \times 10^{-9} + 32.6\mu^2)\sqrt{m} \cdot v, \\ A_1 &= 237.72 + K_w(1 + 11.50 \times \mu^2) + K_p(11.5 + 237.72 \times \mu^2) \\ &\quad + \mathfrak{R}^2(58.91 + 1189.56 \times \mu^2) - v^2(11.5 + 337.72 \times \mu^2), \\ A_2 &= -\mathfrak{R}(132.55 + 2716.7 \times \mu^2) + 124.11.r.r_0, \\ A_3 &= 66.26 + 13.68.38 \times \mu^2. \end{aligned} \quad (38)$$

And for C–C conditions:

$$\begin{aligned} A_{-2} &= 1 + 12.30\mu^2, \\ A_{-1} &= (4.94 \times 10^{-9} + 4.75 \times 10^{-4}\mu^2)\sqrt{m} \cdot v, \\ A_1 &= 500.56 + k_w(1 + 12.3 \times \mu^2) + K_p(12.3 + 500.56 \times \mu^2) \\ &\quad + \mathfrak{R}^2(60.21 + 2377.05 \times \mu^2) - v^2(12.3 + 500.56 \times \mu^2), \\ A_2 &= -\mathfrak{R}(143.19 + 5768.5 \times \mu^2) + 3.5 \times 10^{-6}.r.r_0, \\ A_3 &= 75.67 + 3079.12 \times \mu^2. \end{aligned} \quad (39)$$

Eq. (36) is a nonlinear equation with both cubic and quadratic term. To solve this equation and to obtain the nonlinear flow-induced frequency of the SWCNT with an initial imperfection, the MMS is used [52].

In this way, we pinpoint Y in the form $Y \equiv \varepsilon y$, where ε represents a small perturbation parameter. The Eq. (36) can be rewritten as:

$$\begin{aligned} \ddot{y} + 2\mu\dot{y} + y + \varepsilon\alpha_2 \cdot y^2 + \varepsilon^2\alpha_3 \cdot y^3 &= 0, \\ \mu \equiv \frac{A_{-1}}{A_{-2}}, \quad \omega_0^2 \equiv \frac{A_1}{A_{-2}} = 1, \quad \alpha_2 \equiv \frac{A_2}{A_{-2}}, \quad \alpha_3 \equiv \frac{A_3}{A_{-2}}. \end{aligned} \quad (40)$$

To make the damping term $2\mu\dot{y}$ of the same order as the nonlinear terms, γ is defined such that $\mu \equiv \varepsilon^2\gamma$ and the final form of the Eq. (40) will be:

$$\ddot{y} + 2\varepsilon^2\gamma \cdot \dot{y} + y + \varepsilon\alpha_2 \cdot y^2 + \varepsilon^2\alpha_3 \cdot y^3 = 0. \quad (41)$$

Based on the method of multiple scales and to solve the above nonlinear equation, a third-order expansion should be determined. Hence, the time scales are defined as: $T_n = \varepsilon^n t, n = 0, 1, 2$. The approximate solution for Eq. (41) is:

$$y = y_0(T_0, T_1, T_2) + \varepsilon y_1(T_0, T_1, T_2) + \varepsilon^2 y_2(T_0, T_1, T_2) + \dots \quad (42)$$

Substituting Eq. (42) into Eq. (41) and equating each of the coefficients of ε to zero, the perturbation form of Eq. (41) is:

$$\varepsilon^0 : \quad D_0^2 y_0 + y_0 = 0, \quad (43.a)$$

$$\varepsilon^1 : \quad D_0^2 y_1 + y_1 = -2D_0 D_1 y_0 - \alpha_2 y_0^2, \quad (43.b)$$

$$\begin{aligned} \varepsilon^2 : \quad &D_0^2 y_2 + y_2 \\ &= -2D_0 D_1 y_1 - D_1^2 y_0 - \alpha_3 y_0^3 - 2D_0 D_2 y_0 - 2\gamma D_0 y_0 \\ &\quad - 2\alpha_2 y_1 y_0, \end{aligned} \quad (43.c)$$

where $D_n \equiv \partial / \partial T_n$.

The harmonic solution of Eq. (43.a) can be stated as:

$$y_0(T_0, T_1, T_2) = A(T_1, T_2)e^{iT_0} + \bar{A}(T_1, T_2)e^{-iT_0} \quad (44)$$

\bar{A} is the complex conjugate of A and Eq. (43.b) becomes:

$$\begin{aligned} D_0^2 y_1 + \omega_0^2 y_1 &= (-2iD_1 A e^{iT_0} + 2iD_1 \bar{A} e^{-iT_0}) \\ &\quad - \alpha_2 [A^2 e^{2iT_0} + 2A \cdot \bar{A} + \bar{A}^2 e^{-2iT_0}]. \end{aligned} \quad (45)$$

Eliminating the secular terms from Eq. (45) results in $D_1 A = 0 \Rightarrow A = A(T_2, T_3)$ and the particular solution of Eq. (45) is obtained as:

$$y_1 = \frac{\alpha_2}{3} [A^2 e^{2iT_0} - 8A \cdot \bar{A} + 2A\bar{A} + \bar{A}^2 e^{-2iT_0}]. \quad (46)$$

Substituting Eq. (46) into Eq. (43.c) yields:

$$\begin{aligned} D_0^2 y_2 + \omega_0^2 y_2 &= \left[-2iA' + \frac{10}{3}\alpha_2^2 A^2 \cdot \bar{A} - 3\alpha_3 A^2 \cdot \bar{A} \right] e^{iT_0} + cc \\ &\quad + NST, \end{aligned} \quad (47)$$

where cc and NST stand for the complex conjugate and the non-secular terms, respectively. To eliminate the secular terms, the following condition should be satisfied:

$$-2iA' + \frac{10}{3}\alpha_2^2 A^2 \cdot \bar{A} - 3\alpha_3 A^2 \cdot \bar{A} = 0. \quad (48)$$

By expressing A in polar form $A \equiv \frac{1}{2}a \cdot e^{i\beta}$ where a and β are real values, substituting into Eq. (48), and solving the obtained algebraic equations, a and β are calculated as follows:

$$\begin{aligned} a &= a_0; \quad \beta = \left(\frac{3}{8}\alpha_3 - \frac{5}{12}\alpha_2^2 \right) a_0^2 (T_2 - 2vT_2^2 + \dots) \\ &\cong \left(\frac{3}{8}\alpha_3 - \frac{5}{12}\alpha_2^2 \right) a_0^2 T_2. \end{aligned} \quad (49)$$

Using Eq. (49), the amplitude A is calculated and the harmonic response of the imperfect SWCNT is obtained through Eqs. (44), (46), and (42). Furthermore, the nonlinear frequency ratio Ω can be defined as follows [52]:

$$\Omega = 1 + \varepsilon^2 \sigma, \quad (50)$$

while the detuning parameter σ is obtained as:

$$\sigma \cong \left(\frac{3}{8}\alpha_3 - \frac{5}{12}\alpha_2^2 \right) a_0^2 (1 - 2vT_2 + \dots) \cong \left(\frac{3}{8}\alpha_3 - \frac{5}{12}\alpha_2^2 \right) a_0^2. \quad (51)$$

4. Results and discussion

To gain a better understanding of the computational method, the procedure to determine the analytical solution in the present study has been summarized as a flowchart appeared in Fig. 2.

Based on this procedure, a numerical analysis is conducted to investigate the nonlinear vibrational behavior of a SWCNT conveying fluid with an initially curved imperfection. The nonlinear nature of the flow-induced vibration is analyzed and the effects of several parameters such as the rise of the nanotube, nonlocal parameter, boundary conditions and the mechanical behavior of

the surrounding medium on the nonlinear frequency ratio Ω will be observed.

There are several papers dealing with vibrations of CNTs which assumed the elastic modulus of the SWCNTs to be about 1 Tpa apart from the structural properties [21,23,26,37,43,44,50]. However, molecular dynamics (MD) and molecular mechanics (MM) simulations show that the Young's modulus and the wall thickness of nanotubes vary with the diameter and chirality [53,54]. In this

study, the geometrical and mechanical properties of an armchair (24, 24) SWCNT are employed with Young's modulus of 2.366 Tpa, diameter of 3.0838 nm, and wall thickness of 0.1394 nm as the recent investigation indicates [54] and the aspect ratio of the SWCNT is assumed to be 20. The flowing fluid within the nanotube is assumed to be water. To determine whether the continuum formulations for fluid dynamics could be applied, the dimensionless Knudsen number $K_n = \frac{\lambda}{L}$ is employed. The Knudsen number is

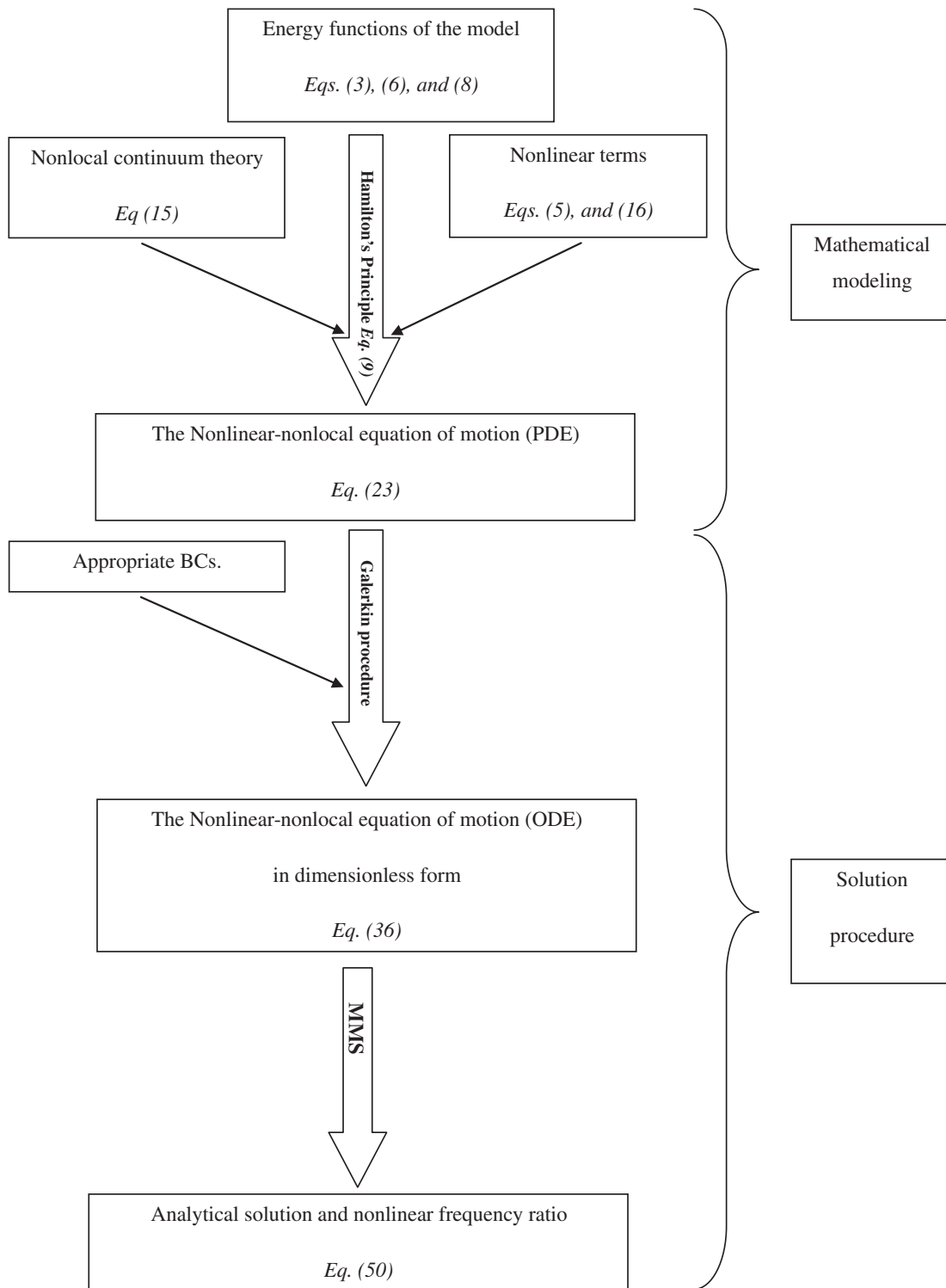


Fig. 2. Computational procedure to determine the analytical nonlinear frequency ratio of the model.

defined as the molecular mean free path length λ to a representative physical length scale L . For an armchair (24, 24) SWCNT conveying water, where λ is 0.28 nm [55] and L defines as the diameter of the nanotube, the Knudsen number is smaller than 0.1. This means that the water can be considered as a continuum medium with the usual mass density of 1000 kg/m³ [56]. Furthermore, the elastic stiffness constant k_w and the shear stiffness constant k_G are set to be zero ($K_w = K_G = 0$).

4.1. Verification of the model

The obtained nonlinear frequency ratio Ω is reduced to the result obtained from the flow-induced vibration of a straight SWCNT conveying fluid through local continuum theory as $\mu = r = 0$. Hence, it will be comparable with the results in Ref. [37]. Fig. 3 represents a comparison between the detuning parameter σ obtained in this study with the one used in Ref. [37]. The detuning parameter σ

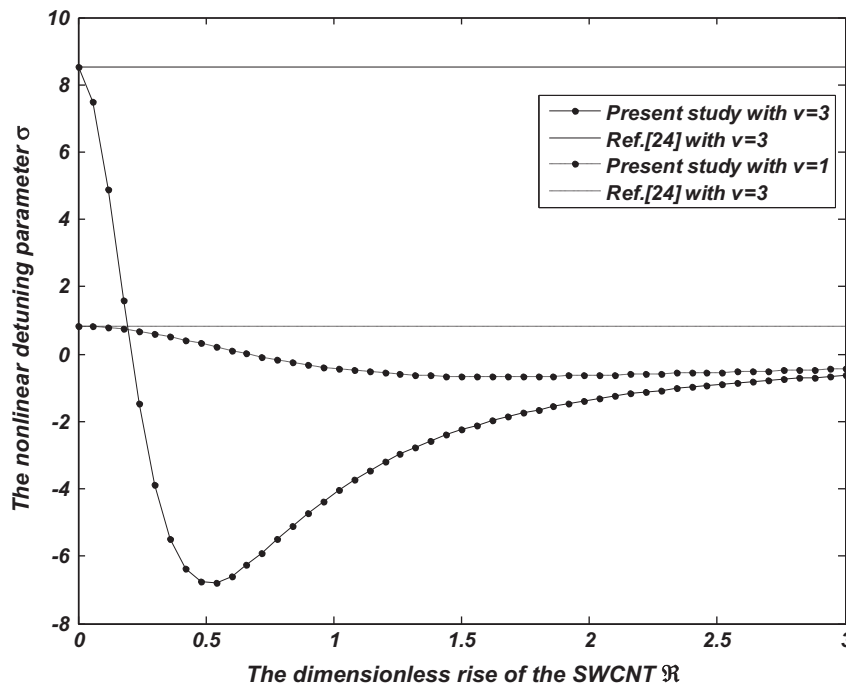


Fig. 3. The nonlinear detuning parameter σ against the dimensionless rise of the SWCNT at two different velocities (a comparison between the present study and Ref. [37]).

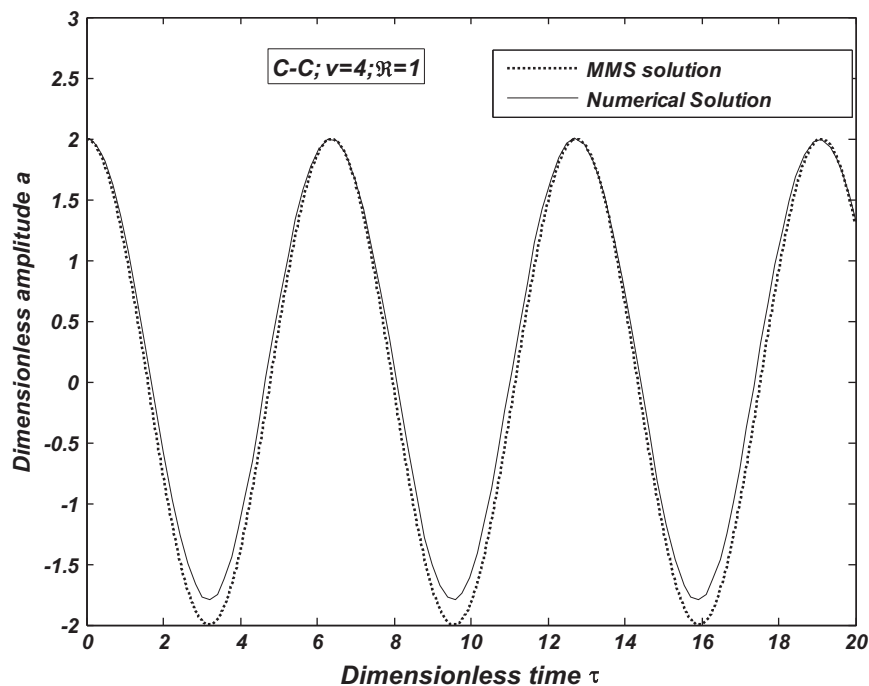


Fig. 4. Comparing the dynamical response of an imperfect SWCNT conveying fluid based on the numerical solution and the multiple scales perturbation solution.

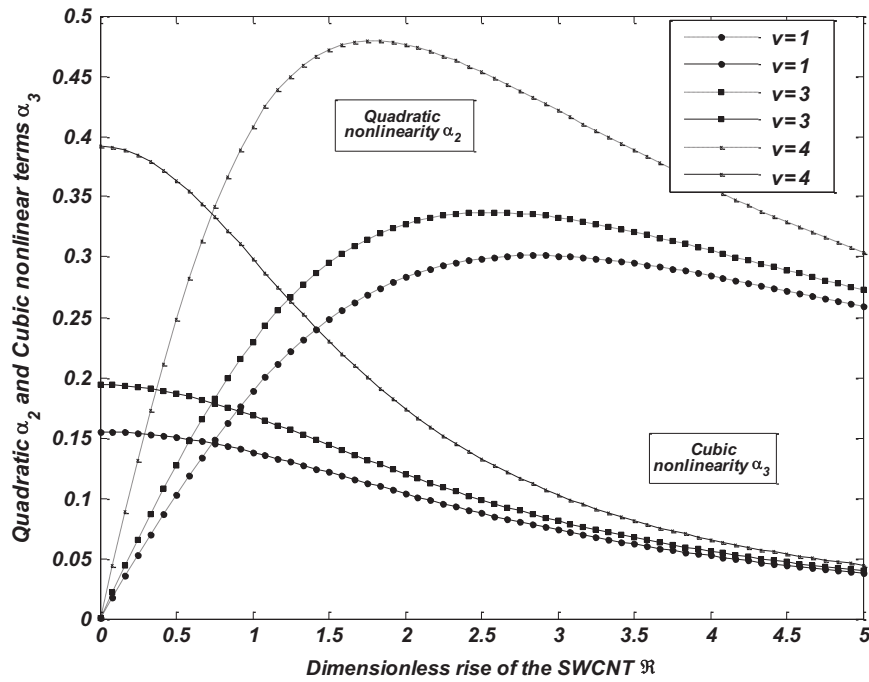


Fig. 5. Quadratic and cubic nonlinear terms (α_2 and α_3) against the dimensionless rise of the SWCNT \mathfrak{R} at several dimensionless flow velocities v .

is plotted against the dimensionless rise \mathfrak{R} for two different dimensionless velocities v . As seen from the figure, as the imperfection of the SWCNT is decreased ($\mathfrak{R} \rightarrow 0$) and the nanotube approaches a straight SWCNT; the detuning parameter σ obtained from the present study and Ref. [37] reaches to the same values. Furthermore, the figure shows that the results in Ref. [37] deviate obviously from the present results by increasing the imperfection of the model or the flow velocity while the flow velocity causes this deviation more effectively.

A second check of the present results is given in Fig. 4. Here, the fourth-order numerical Runge–Kutta method is used to represent the numerical solution of the nonlinear governing equation of the model (Eq. (41)). The Matlab subroutine *ode45* is used to solve the differential equation since it is recommended in the Matlab manual to be the first choice due to its accuracy. The obtained dynamical behavior and the numerical result of the nanotube midpoint displacement are compared with the MMS analysis results and as can be seen, the multiple scales results keep a good

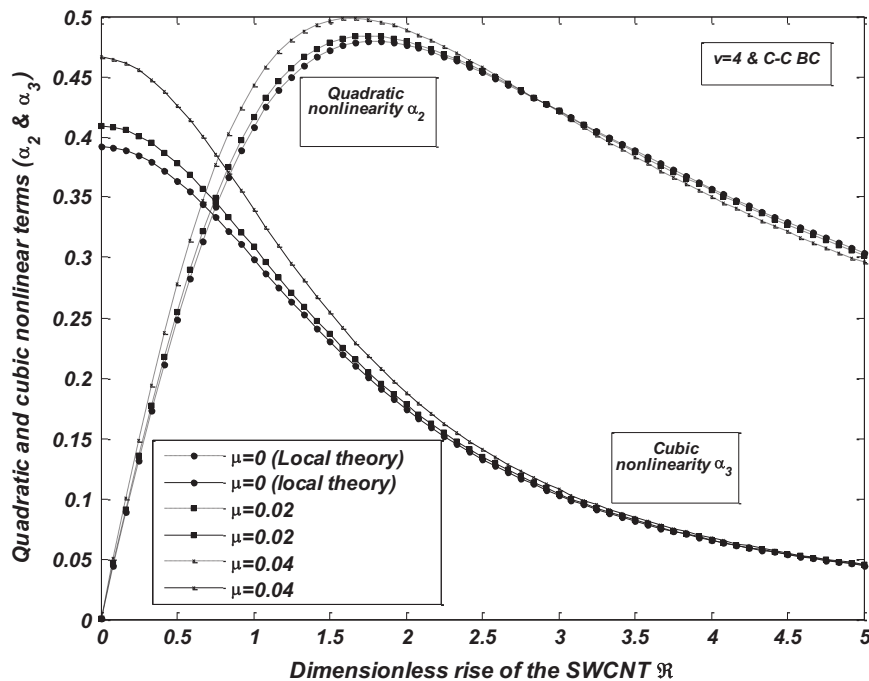


Fig. 6. Quadratic and cubic nonlinear terms (α_2 and α_3) against the dimensionless rise of the SWCNT \mathfrak{R} at several dimensionless nonlocal parameters μ .

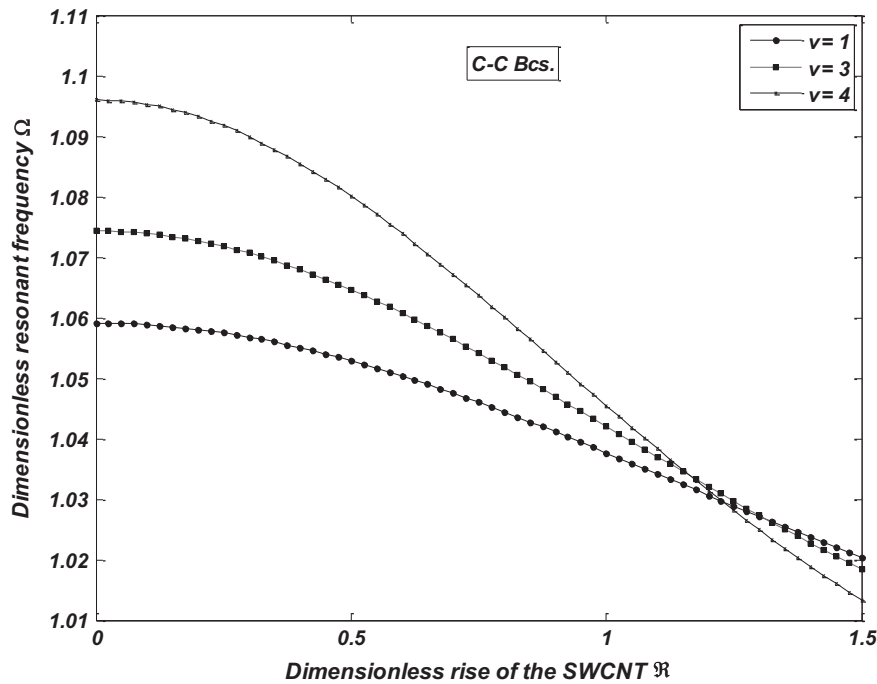


Fig. 7. Nonlinear frequency ratio Ω against the dimensionless rise of the SWCNT \mathfrak{R} at several dimensionless flow velocities ν .

agreement with the numerical exact results and are of high accuracy.

4.2. The nonlinearity of the model

The nonlinear flow-induced problem of a SWCNT conveying fluid with an imperfection is simulated as in Eq. (40). The equation contains both quadratic and cubic nonlinear terms, where α_2 and α_3 are the coefficients represent them, consequently. As previously mentioned, the model covers three different nonlinear phenomena namely the stretching, large deformation, and initial imperfection

or curvature. The cubic nonlinearity α_3 shows the effects of the stretching nonlinearity while the quadratic nonlinear coefficient α_2 stands for both the large deformation and initial curvature. To analyze the nonlinear nature of this problem, the quadratic and cubic nonlinear coefficients (α_2 and α_3) are plotted against the dimensionless rise parameter \mathfrak{R} at various dimensionless flow velocities ν (Fig. 5). As seen in the figure, the quadratic nonlinear coefficient α_2 is strictly related to the rise of the nanotube and the flow velocity. For a slightly curved SWCNT with $\mathfrak{R} < 1.5$, as the initial imperfect rise of curvature is increased, the quadratic nonlinear coefficient α_2 increases sharply, while for $\mathfrak{R} < 1.5$ it

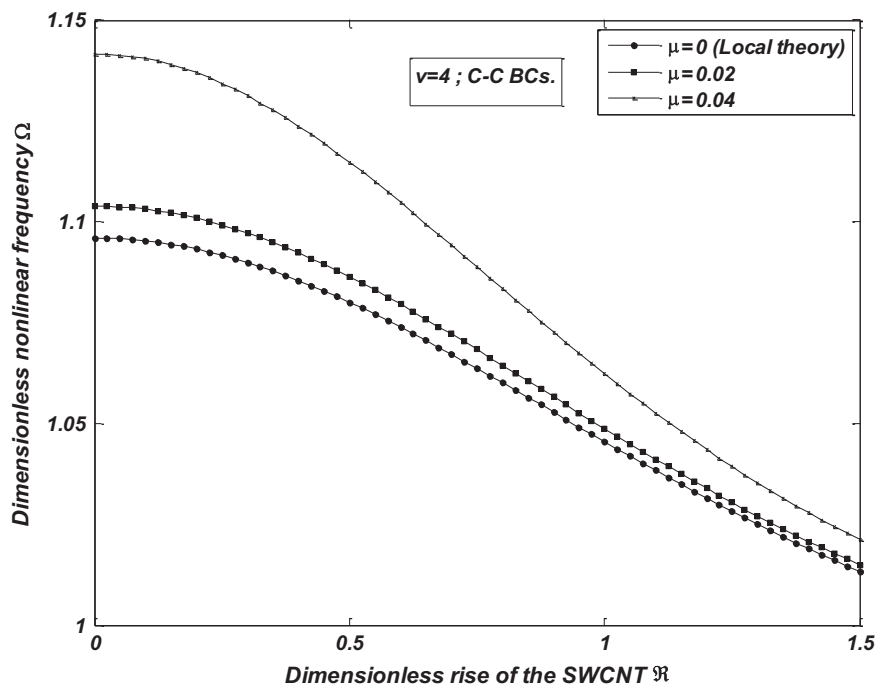


Fig. 8. The nonlinear frequency ratio Ω against the dimensionless rise of the SWCNT \mathfrak{R} for several dimensionless nonlocal parameter $e_0 a$.

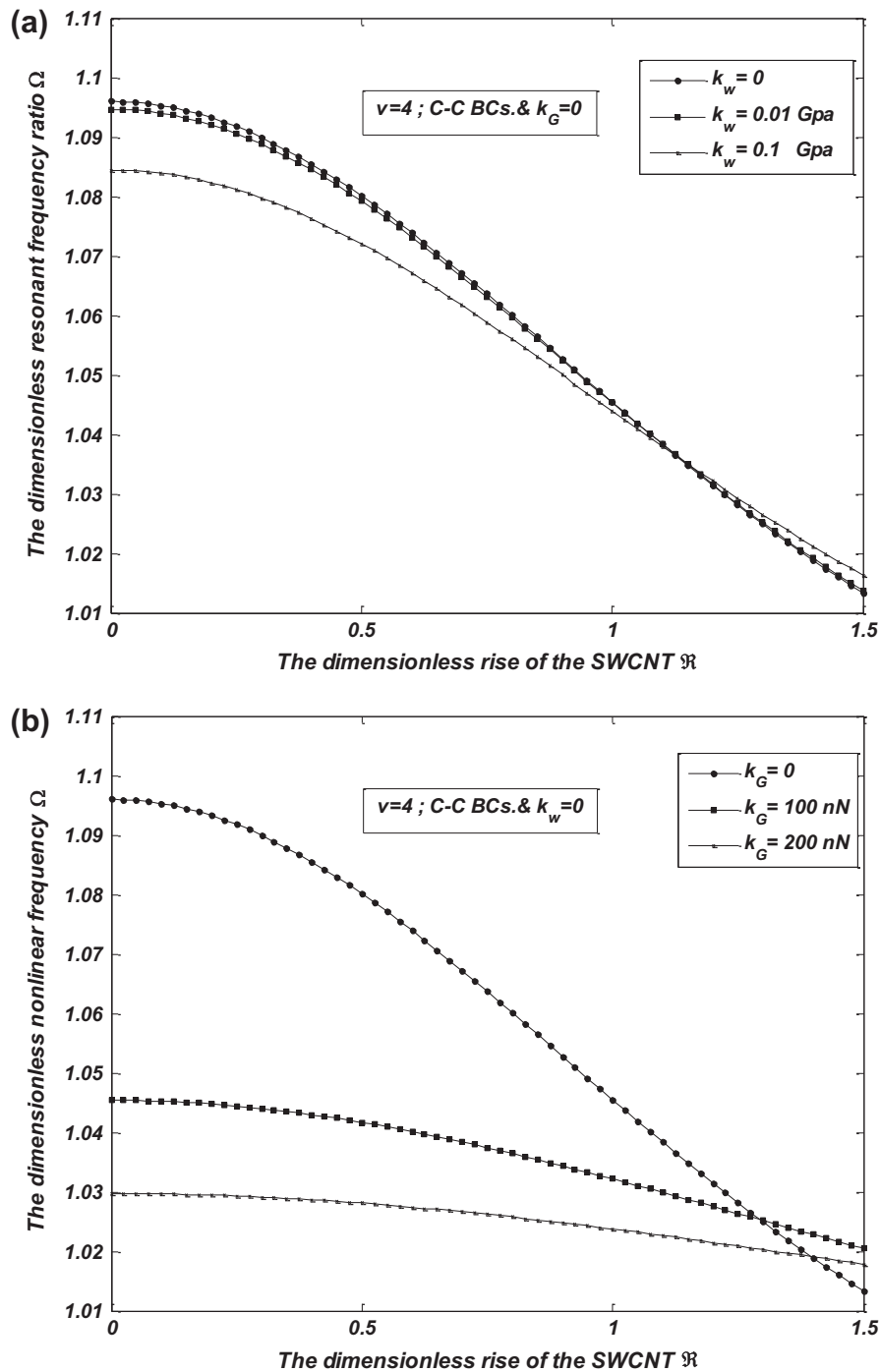


Fig. 9. Nonlinear frequency ratio Ω against the dimensionless rise of the SWCNT \mathfrak{R} (a) for several Winkler stiffness constants k_w and (b) for several Pasternak shear constants k_G .

starts to decrease gradually. Moreover, at higher dimensionless flow velocities v , the quadratic nonlinear coefficient α_2 becomes greater, especially when the dimensionless rise of the SWCNT \mathfrak{R} is about 1.5.

The cubic nonlinear term α_3 varies with the rise of the SWCNT and the flow velocity. Increasing the dimensionless rise of the SWCNT \mathfrak{R} causes the cubic nonlinear term α_3 to decrease while its variation becomes more obvious for $\mathfrak{R} < 1.5$. Furthermore, just like the quadratic nonlinearity α_2 , the cubic nonlinearity of the model increases with an increase in the flow velocity. The figure also depicts a comparison between α_2 and α_3 . As the figure reveals, the numeric value of the quadratic nonlinear term α_2 is always

more than that of the cubic nonlinear term α_3 , and for high values of the dimensionless rise \mathfrak{R} , the nonlinear terms (especially α_3) become almost independent of the dimensionless flow velocity v .

As previously mentioned, in nanostructures, the local continuum models can be modified by the nonlocal elasticity theory. This modification represents a more flexible model as the nanostructure can be viewed as atoms linked by elastic springs while the local model assumes spring constants to take on an infinite value [57]. The nonlocal continuum model can predict the mechanical behavior of a SWCNT provided that the nonlocal parameter e_0a is determined. Since, there is no experimental study to define e_0a for CNTs and to show the effects of the

small-scale parameters, in this study, the dimensionless nonlocal parameter μ is taken to be 0, 0.02 and 0.04 while $\mu = 0$ shows the local continuum model. The nonlocal parameter affects the nonlinearity of the model as Fig. 6 reveals. The nonlinear coefficients (α_2 and α_3) are plotted with the dimensionless rise \mathfrak{R} for several dimensionless nonlocal parameters μ . The importance of the small-scale effects and nonlocal parameter become crucial for small values of \mathfrak{R} ($\mathfrak{R} < 1.5$) and the cubic and quadratic nonlinearity coefficients increase with an increase in dimensionless nonlocal parameter μ . In other words, for slightly curved SWCNT and on the basis of the nonlocal continuum theory, the nonlinearity of the flow-induced behavior of the model becomes more important compared to the theoretically perfect straight nanotube and local continuum theories.

4.3. Nonlinear flow-induced frequency

Nonlocal elasticity has been used to simulate the vibrational behavior of a slightly curved or imperfect SWCNT conveying fluid. The nonlinear flow-induced frequency was calculated using MMS analytically and an explicit expression for the nonlinear frequency ratio Ω was derived. Looking at these Eqs. (50) and (51), it is seen that several parameters influence the nonlinear vibration frequency of the model. Hence, a parametric study is conducted to determine the effects of each individual parameter. In this section, we have focused on the nonlocal parameter, mean flow velocity of the internal flow, the mechanical behavior of the surrounding medium, and the boundary conditions. According to the previous section, and due to the importance of the nonlinear terms in the range $\mathfrak{R} < 1.5$, the dimensionless rise of the nanotube is assumed to be in this range.

Fig. 7 represents the variations of the dimensionless nonlinear frequency ratio Ω with the dimensionless rise of the SWCNT \mathfrak{R} at three different dimensionless flow velocities v for C–C conditions. The figure represents that with increasing the rise of the nanotube, the nonlinear frequency ratio Ω is decreased. This reduction is explained by the fact that with increasing the dimensionless rise of the nanotube \mathfrak{R} , quadratic nonlinearity of the model increases

and the nonlinear detuning parameter σ is decreased accordingly (see Eq. (51)). Moreover, when \mathfrak{R} is smaller than approximately 1 and the CNT has a very slight curvature, the flow velocity becomes a key factor in determining the nonlinear frequency. In this case, the dimensionless nonlinear frequency Ω is increased with flow velocity. However, the nonlinear frequency exhibits a reverse trend in the case of the larger values of \mathfrak{R} ($\mathfrak{R} \gg 1.2$).

As previously mentioned, the nonlinear nature of the model is affected by small-scale effects and the nonlocal parameter. Fig. 8 presents the effects of the dimensionless nonlocal parameter μ on the dimensionless nonlinear frequency Ω with increasing the rise \mathfrak{R} . It is clear that with increasing of the dimensionless nonlocal parameter μ and given a certain value of \mathfrak{R} , the nonlinearity of the model and the corresponding dimensionless nonlinear frequency Ω are increased. This increase is magnified for low values of the rise \mathfrak{R} and the importance of nonlocal elasticity is revealed in the nonlinear flow-induced vibration of a SWCNT with a very slight geometrical imperfection. For instance, when the rise of the model is 1.5, the nonlocal theory (with $\mu = 0.04$) predicts a reduction about 0.008 on the nonlinear frequency ratio Ω compared with the local theory, while as the imperfection of the model is decreased to 0.25, this frequency reduction increases to 0.0426.

The SWCNT is embedded on a Pasternak-type foundation. The mechanical behavior of the foundation is characterized by two different parameters: the elastic stiffness constant k_w and the shear stiffness constant k_G . The effects of the stiffness of the foundation around the SWCNT are shown in Fig. 9. The surrounding medium is assumed to be a polymer matrix with a similar range of parameters k_w and k_G as in Ref. [43]. It can be observed from the results that the dimensionless nonlinear frequency Ω is reduced with increasing the elastic stiffness constant k_w and/or the shear stiffness constant k_G in a certain value of \mathfrak{R} . Furthermore, the slope of the plots is decreased as these parameters are increased. It means that as the elastic medium around the SWCNT becomes stiffer, the nonlinearity of the model and also the sensitivity of the nonlinear frequency to the rise of the nanotube are decreased.

The boundary stiffness can also affect the vibrational behavior of a SWCNT effectively. Since, determining the exact stiffness of

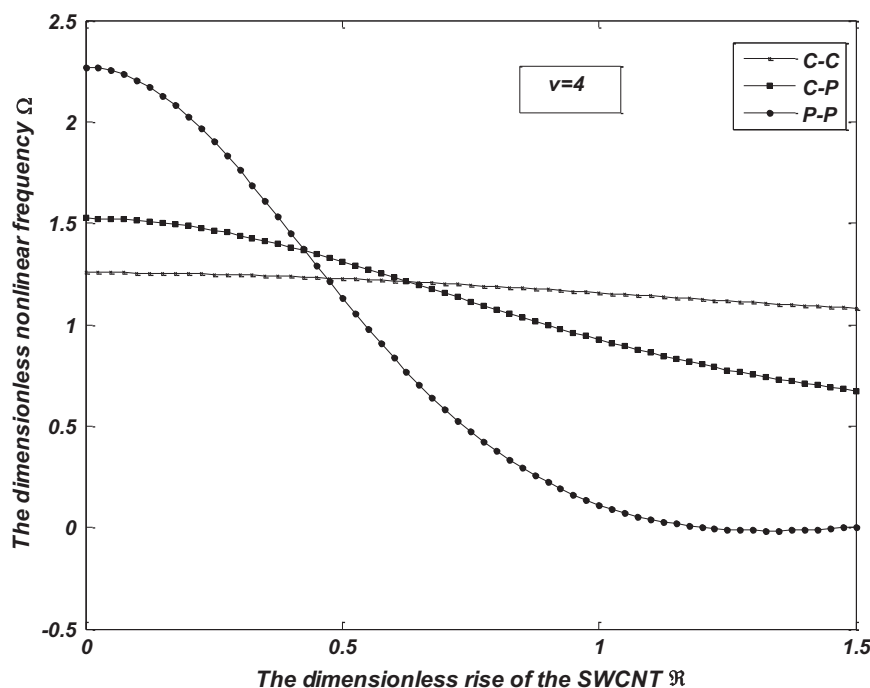


Fig. 10. Nonlinear frequency ratio Ω against the dimensionless rise of the SWCNT \mathfrak{R} with P–P, C–P, and C–C boundary conditions.

the supports of nanostructures is still under dispute [58], the model has been solved for P–P, C–P, and C–C boundary conditions and the variations of the corresponding dimensionless nonlinear frequency Ω with the dimensionless rise \mathfrak{R} are compared in Fig. 10. The results indicate that as the bending stiffness of the nanotube is decreased from C–C to P–P conditions, the variation of the dimensionless nonlinear frequency Ω with the dimensionless rise \mathfrak{R} increases. For example, as the imperfection of the SWCNT rises from $\mathfrak{R} = 0.1$ to $\mathfrak{R} = 1$, the nonlinear frequency ratio Ω is reduced from 2.2060 to 0.117 for P–P boundary conditions and from 1.2548 to 1.157 for C–C conditions, respectively. In fact, as the compliance of the SWCNT due to the boundary conditions is decreased, the nonlinear nature of the model becomes more sensitive to the rise \mathfrak{R} and the decrease of the corresponding nonlinearity will be dramatically magnified. In these cases, the exact determination of the boundary stiffness becomes more crucial in predicting the nonlinear behavior of the flow-induced vibration of a nanotube.

5. Concluding remarks

A SWCNT conveying fluid with an imperfection resting on a Pasternak-type foundation is considered. The imperfection is defined as an initial geometrical curvature and the end conditions are assumed to be immovable causing stretching during the flow-induced vibration. The nonlinear governing equation of motion is derived based on the Eringen's nonlocal theory, and the nonlinearities occur due to the stretching, imperfection and large deformations. An analytical solution has been sought using MMS, and an explicit relation is derived for the nonlinear frequency ratio. The model displays good agreements with the numerical solution and with the previous literature. The results show that on the basis of the nonlocal theory and at high flow velocities, nonlinearity of the model become more important, especially for a slightly curved SWCNT. Moreover, the geometrical imperfection causes the nonlinear frequency ratio to decrease while increasing the flow velocity and the nonlocal parameter with a decrease in the bending stiffness of the model, due to the foundation or to the boundary conditions, make the model more nonlinear and increase the nonlinear frequency ratio.

6. Future outlook

Carbon nanotubes, among several other applications, can be used as nano-pipes to transport fluids and gases on the nano-scale. This potential application makes nanotubes appropriate promising candidates for several interesting nanofluidic devices. Targeted DDSs (especially in cancer therapy), nano-pipettes, nano-syringes, and hydraulic nano-actuators will be designed and applied by using CNTs in the near future. For this purpose and according to our obtained results, the dynamical behavior of CNTs conveying fluid and the fluid–structure interaction should be considered precisely in modeling and simulating of these devices. Meanwhile, the nonlinear phenomena such as large deformations, stretching, and geometrical imperfections may play important roles on the operational conditions of these nano-equipments and should not be neglected during the designing process, consequently.

References

- [1] S. Iijima, *Nature* 354 (6348) (1991) 56–58.
- [2] J.C. Charlier et al., *Nanotechnology* 20 (37) (2009).
- [3] S. Mubeen et al., *Analytical Chemistry* 82 (1) (2010) 250–257.
- [4] B. Arash, Q. Wang, V.K. Varadan, *Journal of Nanotechnology in Engineering and Medicine* 2 (2) (2011).
- [5] E. Bichoutskaia et al., *Fullerenes Nanotubes and Carbon Nanostructures* 18 (4–6) (2010) 523–530.
- [6] K. Eom et al., *Physics Reports* 503 (4–5) (2011) 115–163.
- [7] M. Lu et al., *Journal of Micromechanics and Microengineering* 20 (10) (2010).
- [8] C.H. Ke et al., *Journal of the Mechanics and Physics of Solids* 53 (6) (2005) 1314–1333.
- [9] Y.E. Lozovik, A.V. Minogin, A.M. Popov, *Physics Letters Section A: General Atomic and Solid State Physics* 313 (1–2) (2003) 112–121.
- [10] X. Dong et al., *Journal of Physical Chemistry C* 112 (26) (2008) 9891–9895.
- [11] M. Hamdi et al., *Rotary nanomotors based on head-to-head nanotube shuttles*, Anchorage, AK, 2010.
- [12] F. Delogu, *Journal of Physical Chemistry C* 113 (36) (2009) 15909–15913.
- [13] R.A. Freitas Jr., *Journal of Computational and Theoretical Nanoscience* 2 (1) (2005) 1–25.
- [14] S.S. Hosseini Yazdi, M.M. Mashadi, *Journal of Applied Sciences* 7 (5) (2007) 715–719.
- [15] S.J. Teng, J.N. Wang, X.X. Wang, *Journal of Materials Chemistry* 21 (14) (2011) 5443–5450.
- [16] C.D. Reddy et al., *Applied Physics Letters* 90 (13) (2007).
- [17] A. Noy et al., *Nano Today* 2 (6) (2007) 22–29.
- [18] V.S. Saji, H.C. Choe, K.W.K. Yeung, *International Journal of Nano and Biomaterials* 3 (2) (2010) 119–139.
- [19] S.K. Vashist et al., *Carbon* (2011).
- [20] F. Marianna, B. Mukasa, *Nanomedicine: Nanotechnology, Biology, and Medicine* 4 (3) (2008) 183–200.
- [21] N. Khosravian, H. Rafii-Tabar, *Nanotechnology* 19 (27) (2008).
- [22] J. Yoon, C.Q. Ru, A. Mioduchowski, *Composites Science and Technology* 65 (9 SPEC.ISS.) (2005) 1326–1336.
- [23] J. Yoon, C.Q. Ru, A. Mioduchowski, *International Journal of Solids and Structures* 43 (11–12) (2006) 3337–3349.
- [24] C.D. Reddy, C. Lu, *Journal of Applied Physics* 103 (12) (2008).
- [25] L. Wang et al., *Physica E: Low-Dimensional Systems and Nanostructures* 40 (10) (2008) 3179–3182.
- [26] N. Khosravian, H. Rafii-Tabar, *Journal of Physics D: Applied Physics* 40 (22) (2007) 7046–7052.
- [27] W.J. Chang, H.L. Lee, *Physics Letters, Section A: General, Atomic and Solid State Physics* 373 (10) (2009) 982–985.
- [28] A.C. Eringen, *Journal of Applied Physics* 54 (9) (1983) 4703–4710.
- [29] L. Wang, *Computational Materials Science* 45 (2) (2009) 584–588.
- [30] H.L. Lee, W.J. Chang, *Physica E: Low-Dimensional Systems and Nanostructures* 41 (4) (2009) 529–532.
- [31] H.L. Lee, W.J. Chang, *Journal of Physics Condensed Matter* 21 (11) (2009).
- [32] Y. Zhen, B. Fang, *Computational Materials Science* 49 (2) (2010) 276–282.
- [33] P. Soltani, M.M. Taherian, A. Farshidianfar, *Journal of Physics D: Applied Physics* 43 (42) (2010) 425401.
- [34] D. Walgraef, *The European Physical Journal – Special Topics* 146 (1) (2007) 443–457.
- [35] Y.M. Fu, J.W. Hong, X.Q. Wang, *Journal of Sound and Vibration* 296 (4–5) (2006) 746–756.
- [36] J. Yang, L.L. Ke, S. Kitipornchai, *Physica E: Low-Dimensional Systems and Nanostructures* 42 (5) (2010) 1727–1735.
- [37] M. Rasekh, S.E. Khadem, *Journal of Physics D: Applied Physics* 42 (13) (2009).
- [38] A.Y. Joshi et al., *Journal of Nanotechnology in Engineering and Medicine* 1 (3) (2010) 031004–031005.
- [39] F.T. Fisher, R.D. Bradshaw, L.C. Brinson, *Composites Science and Technology* 63 (11) (2003) 1689–1703.
- [40] W. Xia, L. Wang, *Computational Materials Science* 49 (1) (2010) 99–103.
- [41] E. Ghavanloo, M. Rafiei, F. Daneshmand, *Physics Letters A* 375 (19) (2011) 1994–1999.
- [42] A.K. Misra, M.P. Paidoussis, K.S. Van, *Journal of Fluids and Structures* 2 (3) (1988) 245–261.
- [43] T. Murmu, S.C. Pradhan, *Physica E: Low-Dimensional Systems and Nanostructures* 41 (7) (2009) 1232–1239.
- [44] S.C. Pradhan, T. Murmu, *Journal of Applied Physics* 105 (12) (2009).
- [45] P. Soltani, P. Bahar, A. Farshidianfar, *Proceedings of IMechE. Part C: J. Mechanical Engineering Science* 255 (7) (2011) 1730–1741.
- [46] B.G. Siniir, *Mathematical and Computational Applications* 15 (3) (2010) 490–502.
- [47] O. Aghababaei, H. Nahvi, S. Ziaei-Rad, *International Journal of Non-Linear Mechanics* 44 (2) (2009) 147–160.
- [48] L. Wang, Q. Ni, *Mechanics Research Communications* 36 (7) (2009) 833–837.
- [49] J.N. Reddy, *International Journal of Engineering Science* 45 (2–8) (2007) 288–307.
- [50] J.N. Reddy, S.D. Pang, *Journal of Applied Physics* 103 (2) (2008).
- [51] Y. Fu, J. Zhang, L. Wan, *Current Applied Physics* (2010).
- [52] A.H. Nayfeh, *Introduction to Perturbation Techniques*, Wiley-VCH, Berlin, 1993.
- [53] R.C. Batra, S.S. Gupta, *Journal of Applied Mechanics* 75 (6) (2008) 061010–061016.
- [54] S.S. Gupta, F.G. Bosco, R.C. Batra, *Computational Materials Science* 47 (4) (2010) 1049–1059.
- [55] O. Byl et al., *Journal of the American Chemical Society* 128 (37) (2006) 12090–12097.
- [56] K. Hashemnia, M. Farid, H. Emdad, *Computational Materials Science* 50 (3) (2011) 828–834.
- [57] A. Benzair et al., *Journal of Physics D: Applied Physics* 41 (22) (2008) 225404.
- [58] R.F. Gibson, E.O. Ayorinde, Y.F. Wen, *Composites Science and Technology* 67 (1) (2007) 1–28.